The structure of pore fluids in swelling clays at elevated pressures and temperatures

1999 J. Phys.: Condens. Matter 11 9179

(http://iopscience.iop.org/0953-8984/11/47/305)

J. Phys.: Condens. Matter **11** (1999) 9179–9188. Printed in the UK PII: S0953-8984(99)06787-9

The structure of pore fluids in swelling clays at elevated pressures and temperatures

Ascenso V de Siqueira†, Colin Lobban†, Neal T Skipper†§, Graham D Williams†, Alan K Soper‡, Rob Done‡, John W Dreyer‡, Robin J Humphreys‡ and John A R Bones‡

† Department of Physics and Astronomy, University College, Gower Street, London WC1E 6BT, UK
‡ ISIS Facility, Rutherford Appleton Laboratory, Chilton, Didcot, Oxon OX11 0QX, UK

Received 9 August 1999, in final form 15 October 1999

Abstract. Time-of-flight neutron diffraction has been used in conjunction with isotopic substitution to obtain high-resolution structural data for clay–water–cation systems, at elevated pressures and temperatures. We have developed a new sample environment, that allows us to study clay–fluid interactions *in situ*, under hydrostatic fluid pressures of up to 2 kbar, and temperatures of up to 350 °C. These conditions approximate to those encountered in sedimentary basins, at burial depths of up to 12 km. In this paper we present new results for hydrated clays in which the interlayer cations are magnesium or calcium. We find that throughout our experiments these divalent ions are octahedrally hydrated, as they would be in the bulk. However, hydrogen bonding of interlayer water molecules to the clay surfaces disappears as we approach the critical point. Our data support the assertion that interlayer water is denser than the bulk.

1. Introduction

Swelling clays, such as smectites and vermiculites, are layered aluminosilicates that are widespread in geologic deposits, soils and sedimentary rocks (Grim 1960). They are comprised of stacks of negatively charged mica-like sheets, which are held together by charge balancing interlayer counterions, for example sodium or calcium. Since these counterions have a strong tendency to hydrate, water molecules can be intercalated between the clay layers. This creates an interlayer ionic solution, which causes the clay to swell. Typically, the expanding clay passes through three discrete hydration states, and is then governed by longer-range electrical double layer interactions (Sposito and Prost 1982, Newman 1987).

Detailed knowledge of clay swelling and interlayer fluids is essential if we are to understand many important natural and industrial processes. For example, clay hydration/dehydration plays a key role in subsurface fluid migration, damage to buildings and oil-well collapse (Grim 1960, North 1990). In addition, the interlayer region of clays provides an ideal environment in which to study the fundamental properties of two-dimensional pore fluids.

Recent experimental and computational studies, that take advantage of the methodologies developed during research into bulk ionic solutions, have begun to clarify the ambient structure of fluids in swelling 2:1 clays (Sposito *et al* 1999). The method of neutron diffraction, allied to isotope substitution, has been particularly effective.

§ Corresponding author.

0953-8984/99/479179+10$30.00

Neutron diffraction has already provided definitive structural data for a number of clay–water–cation systems under ambient conditions. Studies of water structure in Li, Na, K and Cs smectites (Cebula *et al* 1979, Hawkins and Egelstaff 1980, Powell *et al* 1997, 1998) argue against a very highly structured interlayer region in rigid association with the silicate sheets. Instead, the data support a liquid-like model, in which cation hydration is similar to that found in aqueous solutions. Higher resolution studies of single crystals of Na and alkylammonium vermiculites (Skipper *et al* 1991, Williams *et al* 1996, 1998) support this view, notwithstanding the higher (tetrahedral) layer charge of the clay sheets. However, a more ordered interlayer is found in Li, Ni and Ca vermiculites (Skipper *et al* 1991, 1994, 1995). The important questions now concern clay–fluid systems under non-ambient conditions, and particularly at the elevated pressures and temperatures encountered in geological settings.

In this paper we describe *in situ* neutron diffraction studies of clay–fluid interactions in Mg- and Ca-substituted smectites and vermiculites, up to 360 °C and 1.8 kbar. In a typical sedimentary basin, these conditions would correspond to a burial depth of about 12 km (North 1990). Our experiments confirm that interlayer water is denser than the bulk, and reveal reversible hydration/dehydration reactions at elevated pressures and temperatures. In addition, isotope substitution of D_2O for H_2O, used in conjunction with difference analysis, has allowed us to construct a detailed picture of the interlayer region. When these data are combined with our previous studies of Na-substituted clays, we obtain unique insight into clay–fluid interactions under geological conditions.

2. Experimental details

We have studied the hydration of two swelling clay minerals. The first is a vermiculite from Eucatex, Brazil, with dry composition: $Si_{6.14}Mg_{5.44}Al_{1.66}Fe_{0.50}Ti_{0.12}Ca_{0.12}O_{20}(OH)_4 \cdot 0.65M^{2+}$ (Newman 1987). This clay occurs naturally as macroscopic crystalline flakes, typically with volume of the order mm^3–cm^3. The second clay is a smectite from Wyoming, USA, with dry composition: $Si_{7.80}Mg_{0.38}Al_{3.48}Fe_{0.34}O_{20}(OH)_4 \cdot 0.31M^{2+}$. This is Source Clay 'SWy-1', obtained from the Source Clays Repository of the Clay Minerals Society (Newman 1987). Because smectites occur only as micron scale particles, we prepared partially aligned cakes of SWy-1, by sedimenting the particles from suspension. Even so, once these samples were immersed in solution, only the (001) Bragg reflection was visible.

From the compositions given above, one can see that the smectites have a lower charge density than vermiculites. In addition, the charge substitution in smectites is predominantly among octahedral cations, and is therefore located at the centre, rather than the surface, of the clay sheets. As a general rule, one would therefore expect interlayer fluids to be more highly structured in vermiculites than smectites.

Given the natural morphology of our samples, our overall strategy was as follows. Single crystals of vermiculite were used to provide detailed information about the microscopic structure of the interlayer region. Smectite particles, which are more widespread in natural and industrial contexts (Grim 1960), were studied to provide macroscopic information, such as the density of interlayer fluid and the location of hydration/dehydration transitions.

The samples were prepared in their homionic forms by repeated soaking in $CaCl_2$ or $MgCl_2$ solution, and were washed free of excess ions in H_2O or D_2O, by hand (vermiculites) or by using dialysis tubing (smectites). During experiments, the clays were immersed in H_2O or D_2O (vermiculites), or 2 M ionic solutions in H_2O or D_2O (smectites).

We have used a purpose-built sample environment, that is able to withstand simultaneously 350 °C and 2 kbar. Samples are contained in the can shown in figure 1, which was manufactured from a 68:32 alloy of Ti and Zr. This alloy has zero coherent scattering (table 1), is chemically

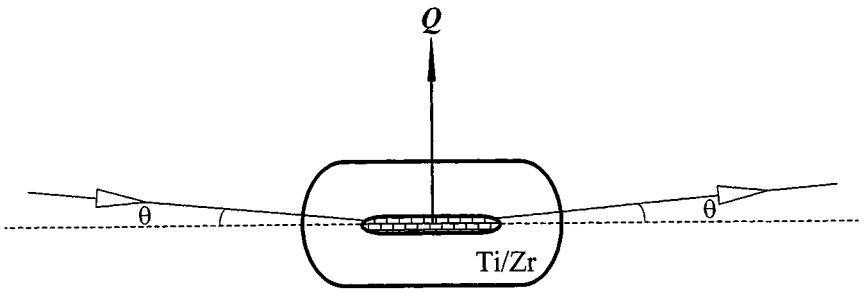

Figure 1. Cross-section of the null scattering Ti/Zr sample container for high pressure/high temperature studies of clay–fluid interactions. The wall thickness of the can is 10 mm. The clay sample is represented by the bricked region, and is oriented so that the c^*-axis is parallel to the scattering vector, $\boldsymbol{Q}$. Pressure is applied hydrostatically via the supernatant fluid, which immerses the clay sample.

Table 1. Neutron scattering lengths, b, for selected species (Lovesey 1984).

Species	b (fm)
H	−3.74
D	6.67
Ca	4.9
Mg	5.38
Fe	9.51
O	5.81
Si	4.15
Al	3.45
Ti	−3.44
Zr	7.16

inert and mechanically strong. The sample is heated by cartridge heaters, inserted into the body of the container above and below the sample itself. Thermocouples are used to monitor and control temperature. Hydrostatic pressure is applied directly through the supernatant fluid, by a hand-pump connected to the sample via high tensile steel piping. The total volume of the working fluid is about 50 cm^3. During the course of an experiment, we achieved sample stability to within 0.2 °C and 10 bar. To reach each state-point, the pressure and temperature were increased simultaneously from the previous values. Due to the finite power of the heaters and the thermal conductivity of Ti/Zr alloy, this process took approximately 15 minutes. After this time, no further equilibration of the sample was required. To confirm that equilibrium had been approached, at least two runs were compared at each state point.

Experiments were conducted on the Liquids and Amorphous Materials Diffractometer, LAD (Howells 1980), at the ISIS pulsed neutron source. In a typical experiment (Skipper *et al* 1991), a clay sample was aligned in the neutron beam so that its c^*-axis was normal to the scattering wavevector, $\boldsymbol{Q}$, of a particular detector (figure 1). Polychromatic pulses of neutrons, with a useable spectrum of wavelengths of between about 0.1 and 5.0 Å, are then directed onto the sample. To cover the full available range of Q in a given experiment, we needed to record two separate data sets for each sample, by scattering into the detectors at $2\theta = 10^\circ$ and $2\theta = 150^\circ$ respectively (figure 2(a)). For microcrystalline smectites, we saw only the first of the (00l) Bragg series. For macrocrystalline vermiculites, on the other hand, we measured approximately 30 of the (00l) Bragg series. We were therefore able to obtain detailed structural information from the latter, as follows.

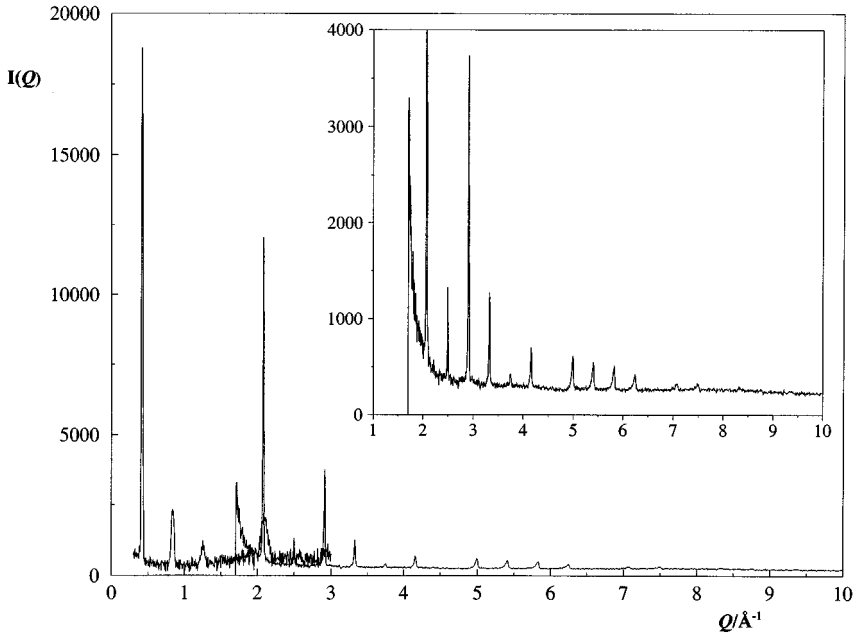

(a)

Figure 2. Neutron scattering intensities from hydrated calcium-substituted clays, showing the (00*l*) Bragg peaks. (a) Ca vermiculite in H_2O at 0 km. Data are shown for the two detector banks at $2\theta = 10$ and 150°, with the latter also expanded as the inset. (b) Ca smectite in a 2 M solution of $CaCl_2$ in H_2O. Data were collected by the detector bank at $2\theta = 10°$. Traces from the bottom are for burial depths of 0.0, 1.5, 3.0, 6.0, 9.0 and 12.0 km. Each curve is displaced by 0.004 units relative to the one below. (c) Ca smectite in a 2 M solution of $CaCl_2$ in D_2O. Data were collected by the detector bank at $2\theta = 10°$. Traces from the bottom are for burial depths of 0.0, 3.0, 6.0, 9.0 and 12.0 km. Each curve is displaced by 0.004 units relative to the one below. We assume pressure and temperature gradients of 150 bar km^{-1} and 30 °C km^{-1} respectively.

Raw diffraction data were corrected for absorption and multiple scattering, and normalized by reference to the incoherent scattering from a vanadium standard (Skipper *et al* 1991). The corrected intensity, $I(Q)$, then contains the basal plane (00*l*) Bragg reflections. These intensities are related to the neutron scattering along the c^*-axis, $\rho(z)$, via the structure factor $F(Q)$

$$I(Q) = M(Q)|F(Q)|^2 \tag{1}$$

$$F(Q) = \int_{-d/2}^{d/2} \rho(Z)[\cos(Qz) + \mathrm{i}\sin(Qz)]\,\mathrm{d}z \tag{2}$$

where d is the clay layer spacing. $M(Q)$ is a Q-dependent form factor that takes into account the effects of mosaic spread, finite sample size and the Debye–Waller factor (Skipper *et al* 1991).

For each set of conditions, data are collected for two samples containing H_2O and D_2O respectively. Due to this application of H/D isotope substitution, separate neutron scattering profiles can be obtained for hydrogen and other species (Skipper *et al* 1991). This is achieved by simultaneous Monte Carlo simulation of the two isotopically distinct integrated intensities, as follows.

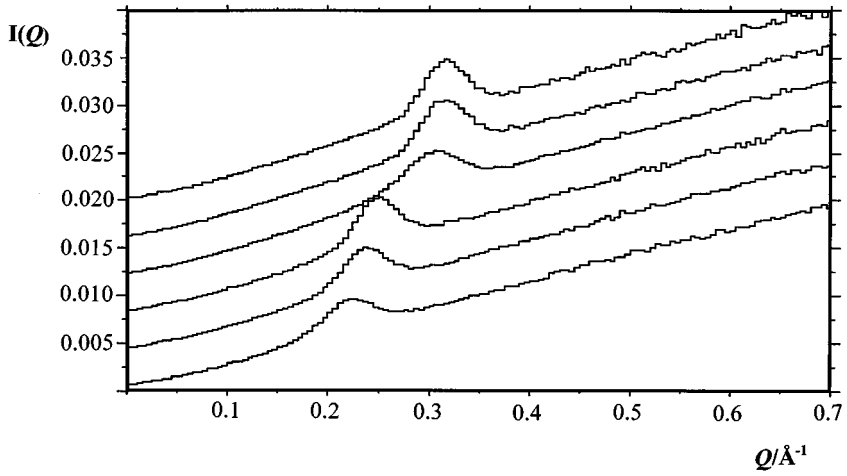

(b)

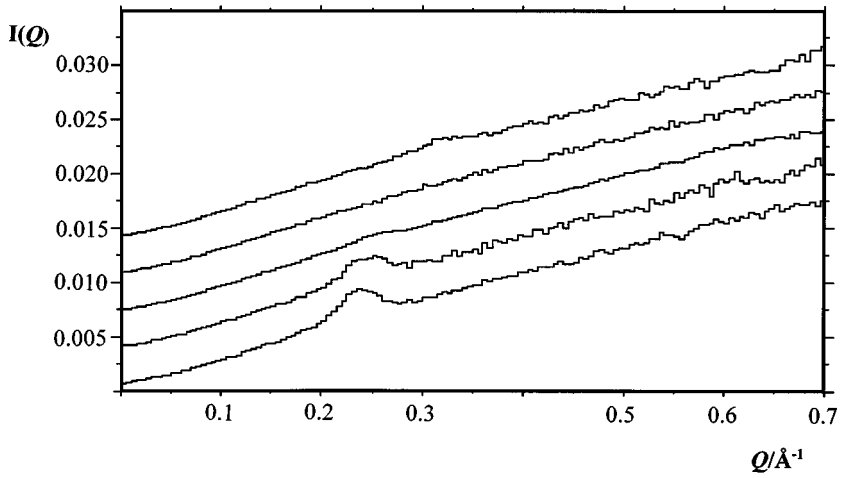

(c)

Figure 2. (Continued)

Two arrays are set up, $\rho(z)_1$ and $\rho(z)_2$, each containing 200 moveable 'particles'. Every particle is associated with a Gaussian distribution of neutron scattering density. The two arrays are combined to produce neutron scattering density profiles representing the hydrogenated and deuterated samples.

$$\rho(z)_H = \rho(z)_1 + b_H\rho(z)_2 \qquad \text{and} \qquad \rho(z)_D = \rho(z)_1 + b_D\rho(z)_2 \tag{3}$$

where b_H and b_D are the scattering lengths of hydrogen and deuterium respectively (table 1). Typically, the total R-factor for the fit to the two sets of corrected intensities was about 3%.

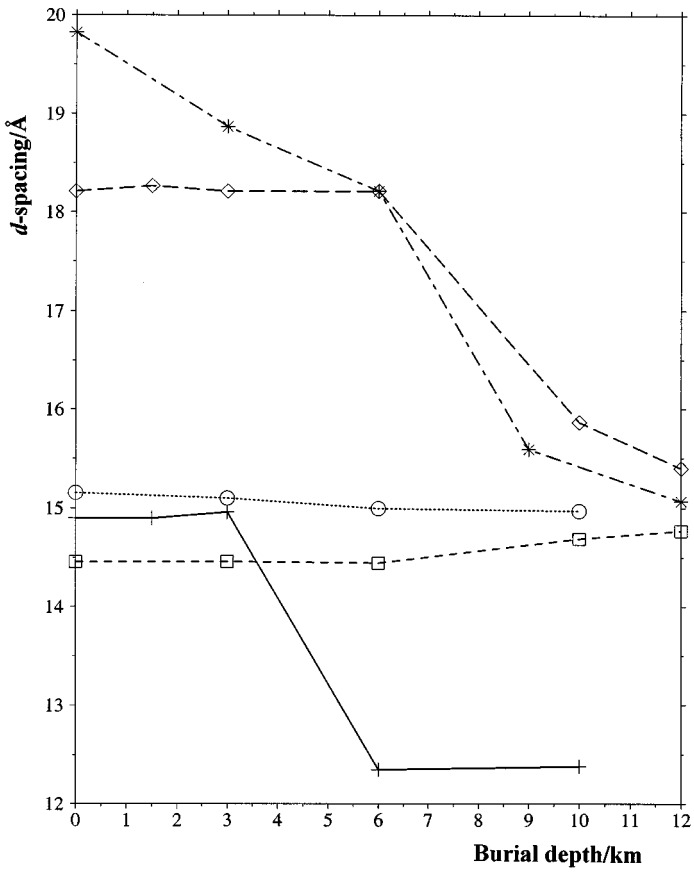

Figure 3. Hydration state of swelling clays as a function of burial depth. Ca smectite, dot–dashed line and stars; Na-smectite, long-dashed line and diamonds; Ca vermiculite, dotted line and circles; Na vermiculite, solid line and pluses; Mg vermiculite, dashed line and squares. In calculating burial depth we assume pressure and temperature gradients of 150 bar km^{-1} and 30 °C km^{-1} respectively.

3. Results and discussion

3.1. Smectite and vermiculite clay hydration

We have followed the hydration of our clays along a typical 'burial' curve, in which the geostatic pressure gradient is 150 bar km^{-1} and the geothermal temperature gradient is 30 °C km^{-1} (North 1990). Our maximum 'depth' was 12 km, corresponding to 1.8 kbar and 360 °C.

We show typical neutron scattering intensities, $I(Q)$, in figures 2(a)–2(c). The position and spacing of the (00l) Bragg peaks tell us immediately the d-spacings of the clay layers. These are presented, as a function of burial depth, in figure 3. To interpret these data, we recall that the clay layers themselves are 6.56 Å thick, and that the d-spacing of dry clays is about 9.8 Å (Newman 1987). If one assumes that the radius of a water molecule is 2.7 Å, clay hydrates containing one, two and three molecular layers of water will have d-spacings of around 12.5, 15.2 and 17.9 Å.

We first consider Ca and Na smectite (the latter has already been discussed in Skipper *et al* 1999). Under ambient conditions these samples exist as our (loosely defined) three-layer

hydrates, with d-spacings of 19.82 Å (Ca) and 18.21 Å (Na). Since both Ca^{2+} and Na^{+} have a hydrated radius of 2.4 Å (Enderby *et al* 1987, Ohtaki and Radnai 1993), we attribute the relatively large value found in Ca smectite to the existence of a distinct second hydration shell around Ca^{2+}. This shell will be disrupted by the increasing temperature it encounters during burial, and at 6 km burial the two curves coincide at 18.21 Å. This point (180 °C and 900 bar) is the limit of stability of the three-layer hydrate. The two-layer hydrate is observed at 9 km, but, interestingly, the Ca smectite now has a lower d-spacing than the Na smectite: hydrated Ca^{2+} presumably acts as a link between adjacent clay layers, pinning them together (Skipper *et al* 1994). Finally, we note that for all the two-layer hydrates the d-spacings converge towards 15 Å at the critical point (which occurs at about 13 km). This observation implies that at high temperatures the clay layer spacing is determined primarily by the radius of the water molecules, rather than the solvated cations.

Hydration/dehydration reactions have previously been observed in smectites, by using x-ray diffraction techniques (Colten 1986, Huang *et al* 1994, Wu *et al* 1997). This research has mapped out the clay layer spacing, as a function of external fluid density and temperature. For Na and Ca smectite, these authors place the conversion of three- to two-layer hydrates at 310–380 °C and 260–350 °C respectively. Our data suggest a transition temperature of 240 °C (at 8 km). There are two reasons why we might expect this difference. First, our experiments used 2 M ionic solution, rather than pure water, as the working fluid. Second, we believe that we have probably worked at lower fluid pressures than the researchers using closed x-ray diffraction cells. For the latter, pressure is calibrated by assuming the same fluid density in the clay and in the surrounding bulk. In fact, it is known that increased pressure suppresses dehydration reactions (van Groos and Guggenheim 1984, Hall *et al* 1986). This leads to the important conclusion that fluid (water) density is, in fact, greater in the clay than in the bulk. We are now in a position to test this hypothesis directly.

We have conducted experiments using both H_2O and D_2O in the supernatant fluid. In figure 2(c), we present $I(Q)$ data for Ca smectite immersed in a 2 M solution of $CaCl_2$ in D_2O, as a function of burial depth. We see that the (001) Bragg intensity decreases with burial depth, and is absent at 9 km (contrast this with the equivalent data for H_2O, shown in figure 2(b)). From equations (2) and (3), this implies that at 9 km the average neutron scattering density is equal within the clay layers and interlayer region. From the known composition of the smectite sheets, and assuming that the solid–liquid interface occurs 4.15 Å from the centre of the clay sheets, we obtain the water content of 9.9 water molecules per O_{20} structural unit, or 240 mg/g clay. This compares with a value of 230 mg/g clay, at 80% relative humidity and 25 °C (Keren and Shainberg 1975). The density of water is then given by

$$\rho(N) = \frac{Nm}{V(N) - V(0)} \tag{4}$$

where N is the water content in molecules per structural unit, m is the mass of a water molecule and $V(N)$ is the volume of the smectite structural unit containing N water molecules. We therefore arrive at $\rho(9.94) = 1.06\,\mathrm{g\,cm^{-3}}$, which can be compared with a value of $0.874\,\mathrm{g\,cm^{-3}}$ in the bulk at this pressure and temperature (Haar *et al* 1984). Our data are therefore consistent with the theory that interlayer water is denser than the bulk (van Groos and Guggenheim 1984, Hall *et al* 1986, Siqueira *et al* 1997).

Turning now to vermiculites, we see that the Ca- and Mg-substituted samples are stable as two-layer hydrates. Previous experiments conducted under ambient conditions have shown that octahedrally hydrated divalent cations pin adjacent clay surfaces together (Skipper *et al* 1991, 1994). The hydrated radii of Mg^{2+} and Ca^{2+} are 2.05 and 2.40 Å respectively (Enderby *et al* 1987, Ohtaki and Radnai 1993), and are therefore consistent with the 0 km d-spacings of 14.49 Å (Mg vermiculite) and 15.18 Å (Ca vermiculite). As depth is increased, and we

approach the critical point, we again observe convergence towards a *d*-spacing of about 15 Å. This is consistent with our previous comments concerning smectite hydrates. Interestingly, the asymptote implies an increase in layer spacing for Mg vermiculite during burial, and a decrease for Ca vermiculite.

A final note on our vermiculite hydration data relates to the isotope effect, due to substitution of D_2O for H_2O. The deuterated samples produced *d*-spacings that were consistently larger than their hydrogenated counterparts (of the order of 0.02 Å). We attribute this to an increase in the water content of the former, due to a reduction in the entropic cost of intercalation on going from H_2O for D_2O.

We have discussed the data for Na vermiculite in a previous paper (Skipper *et al* 1999). In brief, during 'burial' we first note a small expansion of this spacing. On further burial, we observe reversible dehydration from a two- to a one-layer hydrate. This reaction coincides with observed disruption of the cation solvation.

Although our main sequence of experiments followed a 'burial' curve, at the end of this series we did measure the clay-layer spacing at various strategic points on the way back up to the 'surface' (unfortunately, this rehydration series was limited by the available beam-time). We observed no appreciable hysteresis in the clay-layer spacing. However, there was an overall decrease in peak intensities, presumably due to an increase in the mosaic spread of the sample. The former observation is consistent with previous x-ray experiments, conducted at elevated pressures and temperatures and with relatively low fluid densities (Colten 1986, Huang *et al* 1994).

3.2. Interlayer structure in vermiculite clays

Neutron scattering density profiles were obtained from integrated intensities of the (00*l*) series of Bragg peaks, using equations (1)–(3). Due to our use of H/D isotope substitution, we were able to locate unambiguously the protons in our systems. In figures 4(a) and 4(b), we present two sets of density profiles, obtained from Ca vermiculite at burial depths of 0 and 10 km. The former are consistent with our earlier experiments on calcium substituted Llano vermiculite (Skipper *et al* 1994).

At 0 km one can clearly see clay-layer density peaks at 0.0, 1.0, 2.7 and 3.28 Å (solid curve). These correspond to the octahedral cations, apical oxygen atoms, tetrahedral cations and basal plane oxygen atoms respectively. The solid line peak at 6.0 Å is due to oxygen atoms of the interlayer water molecules. The central peak at 7.4 Å can be assigned to the interlayer Ca^{2+} counterions. There are six oxygen atoms per counterion, suggesting an octahedral coordination sphere.

If one turns to the hydrogen density (dotted line), one can see interlayer peaks at 5.1 and 6.2 Å. These show that the water molecules are strongly hydrogen bonded to the clay surface. Interestingly, we also see hydrogen density within the clay layers, at about 3 Å. This density implies that water molecules, most probably in the form of H_3O^+ (Skipper *et al* 1991), are attached to the clay surface, and are ready to take part in diagenetic reactions.

Our data obtained at 10 km provide the first detailed picture of pore water under sub-surface conditions. Importantly, there is no significant change in the scattering from within the clay sheets. This implies that no diagenetic reactions have taken place during our experiments, consistent with the overall reversibility of our 'burial'. The interlayer region still shows (broadened) peaks in the oxygen density, at around 6.0 Å. However, we can no longer resolve separate proton peaks at 5.1 and 6.2 Å. It is important to note, however, that the proton density still lies between 4.5 and 6.5 Å, and does not venture into the centre of the interlayer region. This implies that water molecules are still associated with calcium ions,

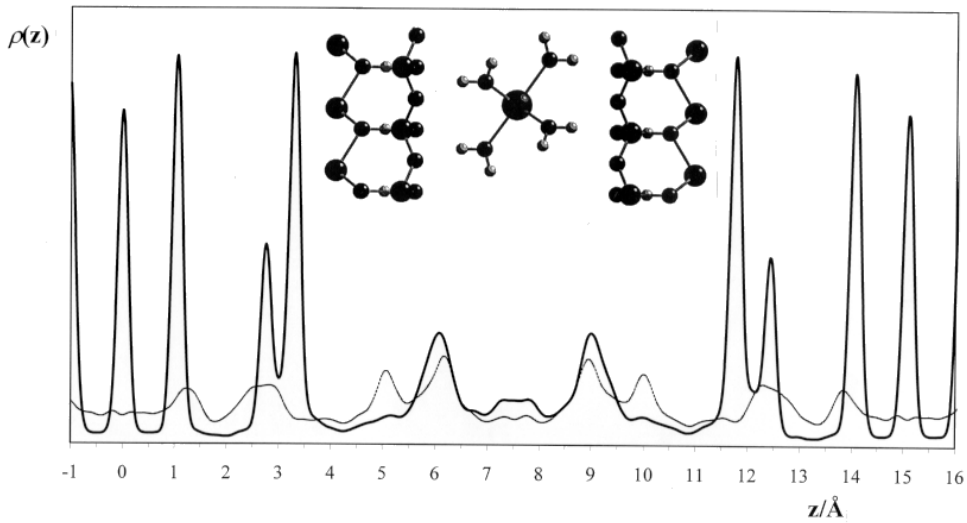

(a)

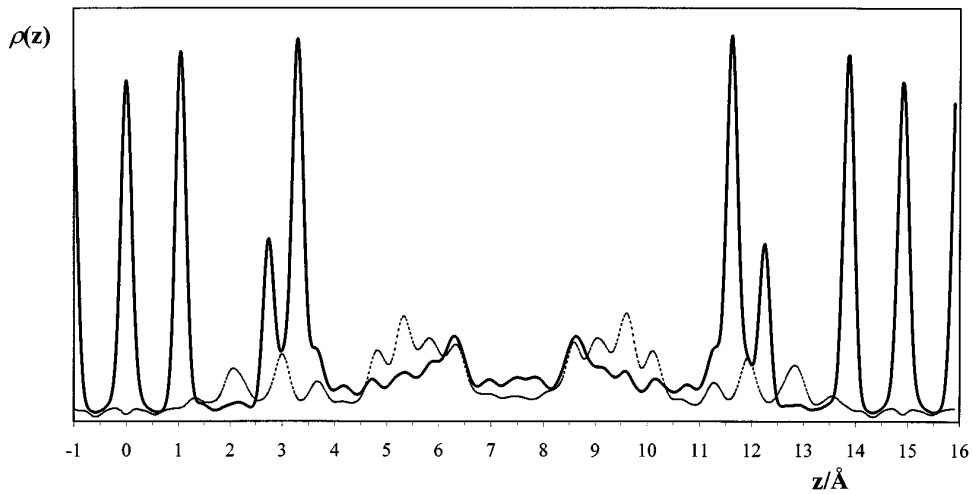

(b)

Figure 4. Normalized neutron scattering densities, $\rho(z)_1$ and $\rho(z)_2$ (equation (3)), for calcium vermiculite at burial depths of (a) 0 km, with inset showing a $Ca(H_2O)_6^{2+}$ complex and section of the vermiculite sheet, and (b) 10 km. Due to the application of isotopic labelling of H_2O by D_2O it is possible to separate the interlayer hydrogen/deuterium atoms (dotted line) from all other atoms (bold solid line).

but are rotating freely about the Ca^{2+}–O bond. This sanctity of the calcium coordination is consistent with studies of hydrated nickel ions at supercritical temperatures (Howell and Neilson 1996). We also conclude that the $Ca(H_2O)_6^{2+}$ complexes are still pinned by the clay platelets. This contrasts with our previous observations of Na vermiculite, in which the two- to one-layer transition was preceded by complete loss of interlayer proton structure (Skipper *et al* 1998).

4. Conclusion

Time-of-flight neutron diffraction, in conjunction with isotopic labelling, has been used to provide extremely high-resolution structural data for Mg- and Ca-substituted clay hydrates. A high pressure/high temperature sample environment, constructed from a null scattering alloy of Ti and Zr, has been developed to study clay systems, *in situ* under sedimentary basin conditions. This environment enables us to subject our samples to pressures 2 kbar and temperatures of up to 360 °C, thereby mimicking conditions encountered at depths of up to 12 km beneath the earth's surface.

We conclude that the density of interlayer water exceeds that of the bulk. Calcium and magnesium ions are octahedrally hydrated, as they would be in the bulk, throughout our experiments. However, hydrogen bonding of interlayer water molecules to the clay surfaces disappears as we approach the critical point.

Acknowledgments

We would like to thank the NERC, EPSRC and ISIS Facility for their support of this research.

References

Cebula D J, Thomas R K, Middleton S, Ottewill R H and White J W 1979 *Clays Clay Miner.* **27** 39
Colten V A 1986 *Clays Clay Miner.* **34** 385
Enderby J E, Cummings S, Herdman G J, Neilson G W, Salmon P S and Skipper N T 1987 *J. Phys. Chem.* **91** 5851
Grim R E 1960 *Applied Clay Mineralogy* (New York: McGraw-Hill)
Haar L, Gallagher J S and Kell G S 1984 *NBS/NRC Steam Tables* (New York: Hemisphere)
Hall P L, Astill D M and McConnell J D C 1986 *Clay Miner.* **21** 633
Hawkins R K and Egelstaff P A 1980 *Clays Clay Miner.* **28** 19
Howell I and Neilson G W 1996 *J. Chem. Phys.* **104** 2036
Howells W S 1980 *Rutherford Appleton Laboratory Report* RL-80-017
Huang W-L, Bassett W A and Wu T-C 1994 *Am. Mineral.* **79** 683
Keren R and Shainberg I 1975 *Clays Clay Miner.* **23** 193
Lovesey S W 1984 *Theory of Neutron Scattering from Condensed Matter* (Oxford: Clarendon)
Newman A C D 1987 *Chemistry of Clays and Clay Minerals* (London: Mineralogical Society)
North F K 1990 *Petroleum Geology* (Boston, MA: Unwin Hyman)
Ohtaki H and Radnai T 1993 *Chem. Rev.* **93** 1157
Powell D H, Fischer H E and Skipper N T 1998 *J. Phys. Chem.* **102** 10 899
Powell D H, Tongkhao K, Kennedy S J and Slade P G 1997 *Clays Clay Miner.* **45** 290
Siqueira A V C, Skipper N T, Coveney P V and Boek E S 1997 *Mol. Phys.* **92** 1
Skipper N T, Smalley M V and Soper A K 1994 *J. Phys. Chem.* **98** 942
Skipper N T, Smalley M V, Williams G D, Soper A K and Thompson C H 1995 *J. Phys. Chem.* **99** 14 201
Skipper N T, Soper A K and McConnell J D C 1991 *J. Chem. Phys.* **94** 5751
Skipper N T, Williams G D, Siqueira A V C, Lobban C and Soper A K 1999 *Clay Miner.* at press
Skipper N T, Williams G D, Siqueira A V C, Lobban C, Soper A K, Done R, Dreyer J and Humphreys R 1998 *ISIS Facility Annual Report* (Didcot: Rutherford Appleton Laboratory) p 46
Sposito G and Prost R 1982 *Chem. Rev.* **82** 553
Sposito G, Skipper N T, Sutton R, Park S-H, Soper A K and Greathouse J A 1999 *Proc. Natl Acad. Sci. USA* **96** 3358
van Groos A F K and Guggenheim S 1984 *Am. Mineral.* **69** 872
Williams G D, Skipper N T, Smalley M V, Soper A K and King S M 1996 *Faraday Discuss.* **104** 295
Williams G D, Soper A K, Skipper N T and Smalley M V 1998 *J. Phys. Chem.* B **102** 8945
Wu T-C, Bassett W A, Huang W-L, Guggenheim S and Kooster Van Groos A F 1997 *Am. Mineral.* **82** 69